CHAPTER 3

Observation and Data Analysis

3.1 Sample Galaxies and Data Observation

Data observations were taken with the 2.4 m Thai National Telescope (TNT) at Doi Inthanon, Chiang Mai, Thailand, during 25 - 27 Febuary and 9 - 11 March 2014. we obtained BVR_c broad-band images and [S II], Red-continuum images from the observations. The transmission of all filters are shown in figure B.1. Broad-band observation data were done by using 2048×2048 pixels APOGEE U42 CCD with field of view of 4×4 arc-minute squares. Furthermore, dark, bias and flat images also were obtained for data analysis to reduce noise. Imaging data include 10 pointings covering some field of sky within 20' $\times$ 26', centered on 12h06m +20° 25' as shown in figure 3.1. The observation of each filter was taken with optimize exposure time for each band. The exposure time of the used filter bands were shown in table 3.1.

Table 3.1: Filters and exposure time for the observations.

Filter	exposure time (s)
B	900
V	600
R_c	300
Red-continuum	900
[S II]	900

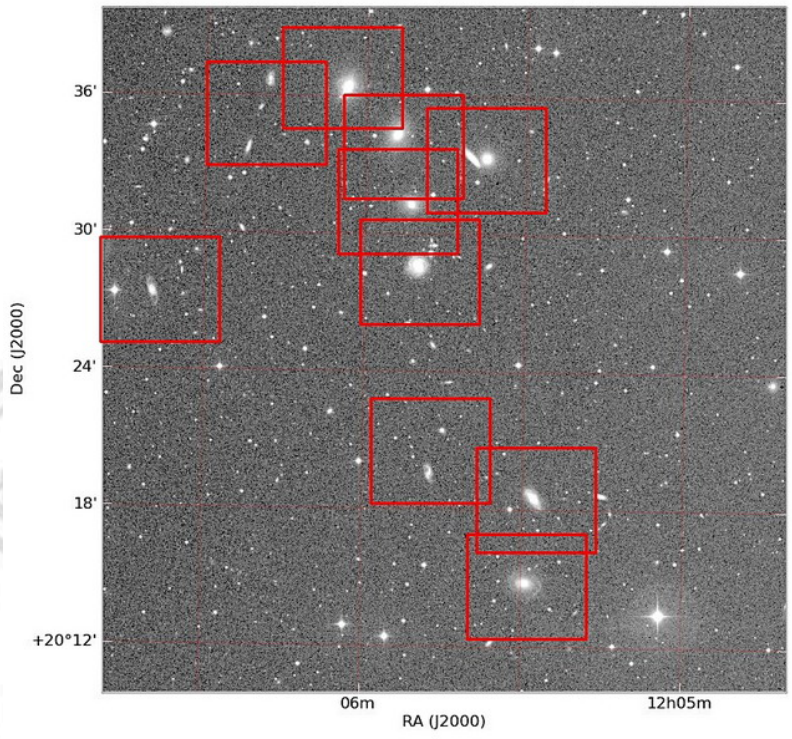

Figure 3.1: The sky area of our observations, including 10 observed frames.

Sample galaxies in this work were selected by using two conditions, one is B magnitude of galaxies less than 20 and the other is the range of recession velocities of galaxies about 6,000 – 8,000 km/s. The lists of sample galaxies as shown in table 3.2.

3.2 Zero Point

Bright stars in frame of images were used to calibrate zero point for all bands. Instrumental magnitudes of the stars were measured by using Starlink package. We used instrumental magnitudes and collected apparent magnitudes from the USNO B1 catalog to calculate zero point for each filter. The calculation of zero point for the B band images is given by

$$zp_{\mathrm{B_j}} = m_{\mathrm{B_j}} - m_{\mathrm{B_{ij}}}, \tag{3.1}$$

where $zp_{\mathrm{B_j}}$ is zero point value of the B band images, $m_{\mathrm{B_j}}$ is apparent magnitude of reference stars in the B band images, $m_{\mathrm{B_{ij}}}$ is instrumental magnitude of reference stars in the B band images. Finally, we averaged zero point values of all stars that are available in all B band images and used this value for calibrated magnitude of galaxies in B waveband. Because

Table 3.2: Sample galaxies in 4095 group which were studied in this work [the NASA/IPAC Extragalactic Database (NED)].

Name	RA	DEC	Velocity (km/s)	Redshift
NGC 4098	12h06m03.9s	+20d36m22s	7296	0.024337
NGC 4095	12h05m54.2s	+20d34m21s	7148	0.023843
NGC 4093	12h05m51.4s	+20d31m19s	7206	0.024037
NGC 4092	12h05m50.1s	+20d28m37s	6719	0.022412
NGC 4091	12h05m40.1s	+20d33m21s	7686	0.025638
NGC 4089	12h05m37.4s	+20d33m21s	7267	0.024240
NGC 4090	12h05m27.9s	+20d18m32s	7333	0.024460
NGC 4086	12h05m29.4s	+20d14m48s	7093	0.023660
KUG 1203+206A	12h05m45.0s	+20d21m27s	7589	0.025314
KUG 1203+206B	12h05m47.4s	+20d19m35s	6984	0.023296
VV 062	12h06m18.3s	+20d36m40s	7217	0.024073
SDSS J120621.91+203351.8	12h06m21.9s	+20d33m52s	7214	0.024062
2MASX J12063969+2027235	12h06m39.7s	+20d27m24s	7263	0.024227

numbers of stars in each observed data image are not enough to specify zero point values for each frame. Therefore, the average value of zero point was calculated for whole B band data as follows:

$$ZP_{\mathrm{B}} = \frac{\sum_{j=1}^{N} zp_{\mathrm{B_j}}}{N}, \tag{3.2}$$

where ZP_{B} is averaged zero point of B band images, $zp_{\mathrm{B_j}}$ is zero point values from the calibrated stars and N is the number of the stars in B band images.

Table 3.3: The reference star for calculation of zero points.

USNO No.	RA	DEC	m_{B}	m_{R}	$m_{\mathrm{V_{cal}}}$	$m_{\mathrm{B_i}}$	zp_{B}	$m_{\mathrm{R_i}}$	zp_{R}	$m_{\mathrm{V_i}}$	zp_{V}
1102-0210369	12h05m28.40s	+20d15m26.57s	17.47	16.82	17.11	-13.49	30.96	-13.60	30.08	-14.00	31.11
1105-0205960	12h05m59.05s	+20d31m13.13s	17.07	15.73	16.32	-13.94	31.01	-14.68	30.08	-14.87	31.19
1103-0213143	12h05m53.79s	+20d21m05.32s	17.03	16.39	16.67	-13.79	30.82	-14.26	30.32	-14.55	31.22
1106-0205046	12h06m24.24s	+20d36m27.65s	17.02	16.34	16.64	-14.16	31.18	-14.47	30.48	-14.81	31.45
1102-0210351	12h05m26.91s	+20d17m08.34s	16.94	16.31	16.59	-14.07	31.01	-14.43	30.41	-14.76	31.35
1104-0207684	12h05m55.67s	+20d27m24.18s	16.92	14.76	15.72	-13.99	30.91	-16.03	30.46	-15.63	31.35
1105-0205799	12h05m31.46s	+20d33m17.42s	16.91	16.45	16.65	-13.97	30.88	-14.33	30.44	-14.63	31.29
1103-0213020	12h05m33.43s	+20d20m27.63s	16.83	15.19	15.92	-14.19	31.02	-15.41	30.27	-15.39	31.31
1104-0207795	12h06m33.23s	+20d26m20.70s	16.78	15.51	16.07	-14.49	31.27	-15.12	30.30	-15.30	31.37
1102-0210341	12h05m24.53s	+20d13m41.44s	16.41	15.54	15.93	-14.83	31.24	-15.26	30.47	-15.56	31.49
1105-0205957	12h05m58.60s	+20d34m17.63s	14.7	14.09	14.36	-16.23	30.93	-16.60	30.35	-16.92	31.28
1105-0205875	12h05m47.43s	+20d31m44.13s	14.46	12.94	13.61	-16.44	30.90	-17.67	30.28	-17.64	31.25
1105-0205875	12h05m47.43s	+20d31m44.13s	14.46	12.94	13.61	-16.55	31.01	-17.76	30.37	-17.73	31.34
1105-0205838	12h05m39.22s	+20d32m19.13s	14.43	13.96	14.17	-16.53	30.96	-16.93	30.55	-17.23	31.40
1103-0213016	12h05m32.22s	+20d18m01.73s	13.84	13.36	13.57	-17.37	31.21	-17.56	30.59	-17.91	31.48
1444-01291-1	12h05m47.70s	+20d29m10.07s	13.05	11.47	12.17	-18.16	31.21	-18.81	29.94	-18.96	31.13
Averege							31.03		30.34		31.31

The R band images were carried out by using different filter system with apparent magnitude of catalog. The observations in this study used R Cousins filter system, available R band filter for this observation, that different filter system with the USNO B1, using R Johnson filter system, whereas R calibrated magnitude collected from catalogue is in Johnson system. So, This required correction as follows:

$$zp_{\mathrm{R_j}} = m_{\mathrm{R_j}} - m_{\mathrm{Ri_j}} + \Delta m, \tag{3.3}$$

$$ZP_{\mathrm{R}} = \frac{\sum_{j=1}^{N} zp_{\mathrm{R_j}}}{N}, \tag{3.4}$$

where $zp_{\mathrm{R_j}}$ is zero point value of the R band images, $m_{\mathrm{R_j}}$ is apparent magnitude of reference stars in the R band images, $m_{\mathrm{R_{ij}}}$ is instrumental magnitude of reference stars in the R band images. Δm is difference magnitude of two R band filter systems, ZP_{R} is average zero point of R band images, $zp_{\mathrm{R_j}}$ is zero point values from the calibrated stars and N is the number of the stars in R band images that

$$\Delta m = -2.5 \log(\frac{f_{cousin}}{f_{Jonhson}}), \tag{3.5}$$

where f_{cousin} is the total flux of the Cousin R bandpass and $f_{Jonhson}$ is the total flux of the Johnson R bandpass. The transmission of R Cousins and R Johnson filters are shown in figure B.2.

The apparent magnitudes in V band is not available on database, therefore the V magnitudes were derived from B and R magnitudes. The relation was defined by Greaves [2003], who used about of 20,000 stars to estimated the relationship equation, following equation:

$$m_{\mathrm{Vcal_j}} = 0.444 m_{\mathrm{B_j}} + 0.556 m_{\mathrm{R_j}}, \tag{3.6}$$

and zero point of V band images can be obtained by using equation:

$$zp_{\mathrm{V_j}} = m_{\mathrm{Vcal_j}} - m_{\mathrm{Vi_j}}, \tag{3.7}$$

$$ZP_{\mathrm{V}} = \frac{\sum_{j=1}^{N} zp_{\mathrm{V_j}}}{N}, \tag{3.8}$$

where $m_{\mathrm{Vcal_j}}$ is apparent magnitude for V band from calculation. $zp_{\mathrm{V_j}}$ is zero point value of the V band images, $m_{\mathrm{Vi_j}}$ is instrumental magnitude of reference stars in the V band images, ZP_{V} is averaged zero point of V band images and N is number of stars in V band images. Condition for selection of reference stars was to have enough brightness with B apparent magnitude less than 17.5. With this condition, acceptable uncertainty could be obtained uncertainty. All data of reference stars were listed in table 3.3, such as coordinate of stars, apparent magnitudes, instrumental magnitudes, and zero point in BVR band images.

3.3 The Measurement of Magnitudes and Colors

Surface brightness of galaxies is typically high at the center and decreases as a function of radius. Galaxy's light was measured and interpreted to obtain their physical properties. Thus, the aperture used to measure the properties should cover the light as much as possible and be well defined. A standard aperture is an isophote identified at the surface brightness of 25 B-mag arcsec^{-2}, B_{25} could reach to the faint surface brightness closed to the sky. Several researches were done by using this aperture size. This work used the Extended Surface Photometry (ESP) package of the starlink to determine the B_{25} isophote, getting isophote's diameter, ellipticity and position angle (PA). The aperture for each galaxy was applied to measure galaxy's magnitude for all band images.

3.3.1 Apparent magnitude

Magnitudes of galaxies were estimated by using The Graphical Astronomy and Image Analysis (GAIA) of the Starlink package. The B_{25} isophote, received from the ESP package of the Starlink were used in the GAIA to count number of photons within those apertures. Galaxy count numbers were obtained by subtraction of sky count numbers from total count numbers. The apparent magnitudes were calculated by equations (3.9)-(3.11)

$$B' = ZP_{\mathrm{B}} + B_{\mathrm{i}}, \tag{3.9}$$

$$V' = ZP_{\mathrm{V}} + V_{\mathrm{i}}, \tag{3.10}$$

$$R' = ZP_{\mathrm{R}} + R_{\mathrm{i}}, \tag{3.11}$$

where B', V' and R' are apparent magnitudes of galaxies in B, V and R bands while $B_{\rm i}, V_{\rm i}$ and $R_{\rm i}$ are instrumental magnitudes of galaxies in B, V and R band filter images, respectively.

3.3.2 Galactic extinction correction

For data of the observations, interstellar extinction always affect on brightness of celestial objects. Then, the magnitude values that we got, needed to be corrected. We rectified magnitude values by deduction of the Galactic extinction. The values of the Galactic extinction used in this study were carried from the NASA/IPAC extragalactic database (NED), showing in table 3.4

$$B = B' - A_{\rm B}, \tag{3.12}$$

$$V = V' - A_{\rm V}, \tag{3.13}$$

$$R = R' - A_{\rm R}, \tag{3.14}$$

where B, V and R are apparent magnitudes of galaxies that were corrected already and $A_{\rm B}$, $A_{\rm V}$ and $A_{\rm R}$ are the Galactic extinction in B, V and R bands, respectively.

Table 3.4: The Galactic extinction of sample galaxies from NED

Name	Galactic Extintion		
	B	V	R
NGC 4098	0.12	0.091	0.072
NGC 4095	0.121	0.091	0.072
NGC 4093	0.115	0.087	0.069
NGC 4092	0.111	0.084	0.066
NGC 4091	0.123	0.093	0.074
NGC 4089	0.123	0.093	0.074
NGC 4090	0.135	0.102	0.081
NGC 4086	0.136	0.103	0.081
KUG 1203+206A	0.116	0.087	0.069
KUG 1203+206B	0.12	0.091	0.072
VV 062	0.112	0.085	0.067
SDSS J120621.91+203351.8	0.116	0.088	0.07
2MASX J12063969+2027235	0.134	0.101	0.08

3.3.3 Absolute magnitudes

We used apparent magnitude to compute absolute magnitude as relation are shown by

$$M_{\mathrm{B}} = B - 5\log d + 5, \tag{3.15}$$

$$M_{\mathrm{V}} = V - 5\log d + 5, \tag{3.16}$$

$$M_{\mathrm{R}} = R - 5\log d + 5, \tag{3.17}$$

where M_{B}, M_{V} and M_{R} are absolute magnitudes of galaxies in B, V and R bands, respectively and d is average distance for this galaxy group.

3.3.4 Color indexes of galaxies

This work has three band magnitudes. Thus, we obtained three colors from difference of apparent magnitudes, i.e. $B-V$, $B-R$ and $V-R$ colors.

3.4 Error of Magnitudes and Color Indexes

Since the apparent magnitudes of galaxies were determined from zero point and instrumental magnitudes. Therefore, error of magnitudes were calculated by

$$\sigma(B)^2 = \sigma(ZP_{\mathrm{B}})^2 + \sigma(B_{\mathrm{i}})^2, \tag{3.18}$$

where $\sigma(B)$ is error of B magnitude, $\sigma(ZP_{\mathrm{B}})$ is error of zero point in B band filter images and $\sigma(B_{\mathrm{i}})$ is error of instrumental magnitude in B band filter images. Error of zero point is resulted from standard error of zero point values that were calculated from reference stars in all data images for the same band filters.

$$\sigma(ZP_{\mathrm{B}})^2 = \sigma_{\mathrm{std}}(ZP_{\mathrm{B}})^2 + \sigma_{\mathrm{A}}(m_{\mathrm{B_i}})^2, \tag{3.19}$$

where

$$\sigma_{\mathrm{std}}(ZP_{\mathrm{B}}) = \sqrt{\frac{\sum_{j=1}^{N}(zp_{\mathrm{B_j}} - ZP_{\mathrm{B}})^2}{N(N-1)}}, \tag{3.20}$$

and

$$\sigma_{\mathrm{A}}(m_{\mathrm{B_i}}) = \frac{\sum_{j=1}^{N} \sigma(m_{\mathrm{B_{ij}}})}{N}, \tag{3.21}$$

where $\sigma_{\mathrm{std}}(ZP_{\mathrm{B}})$ is standard error of zero point which was calculate from reference stars, $\sigma_{\mathrm{A}}(m_{\mathrm{B_i}})$ is average error of instrumental magnitude of reference stars, $\sigma(m_{\mathrm{B_{ij}}})$ is error of instrumental magnitude of referent stars and N is number of reference stars in B band images. For V and R magnitudes, error values can be calculated by using similar methods of B magnitude. Since effects of convertion of stellar magnitudes in R band and V band were not very large, the error of these effects were neglected.

Color indexes of galaxies were determined from two magnitudes, thus error of color indexes were estimated from error of magnitudes too. Equation for calculation of error was shown by

$$\sigma(B-V)^2 = \sigma(B)^2 + \sigma(V)^2, \tag{3.22}$$

$$\sigma(B-R)^2 = \sigma(B)^2 + \sigma(R)^2, \tag{3.23}$$

$$\sigma(V-R)^2 = \sigma(V)^2 + \sigma(R)^2, \tag{3.24}$$

where $\sigma(B-V)$, $\sigma(B-R)$ and $\sigma(V-R)$ are the error of color.

Table 3.5: The apparent magnitude and error of sample galaxies.

Name	B	$\sigma(B)$	V	$\sigma(V)$	R	$\sigma(R)$
NGC 4098	14.22	0.03613	12.88	0.04468	13.21	0.02850
NGC 4095	14.30	0.03611	13.59	0.04469	13.38	0.02848
NGC 4093	15.02	0.03629	14.33	0.04473	14.12	0.02852
NGC 4092	14.11	0.03607	13.58	0.04469	13.42	0.02848
NGC 4091	14.69	0.03602	14.04	0.04468	13.81	0.02846
NGC 4089	14.53	0.03602	13.81	0.04468	13.59	0.02846
NGC 4090	14.42	0.03604	13.93	0.04469	13.77	0.02850
NGC 4086	14.53	0.03603	13.91	0.04469	16.79	0.02977
KUG 1203+206A	17.04	0.03706	16.79	0.04521	16.10	0.02923
KUG 1203+206B	16.53	0.03697	16.19	0.04505	15.99	0.03148
VV 062	16.41	0.03704	15.99	0.04625	15.80	0.02950
SDSS J120621.91+203351.8	16.99	0.03744	16.38	0.04622	13.73	0.02849
2MASX J12063969+2027235	15.89	0.03716	15.48	0.04497	15.45	0.02896

Table 3.6: The absolute magnitudes and error of sample galaxies.

Name	M_{B}	$\sigma(B)$	M_{V}	$\sigma(V)$	M_{R}	$\sigma(R)$
NGC 4098	-20.92	0.03613	12.11	0.04468	12.66	0.02850
NGC 4095	-20.84	0.03611	12.81	0.04469	12.71	0.02848
NGC 4093	-20.12	0.03629	13.45	0.04473	13.34	0.02852
NGC 4092	-21.03	0.03607	12.83	0.04469	12.75	0.02848
NGC 4091	-20.45	0.03602	13.20	0.04468	13.07	0.02846
NGC 4089	-20.61	0.03602	13.00	0.04468	12.89	0.02846
NGC 4090	-20.72	0.03604	13.13	0.04469	13.05	0.02850
NGC 4086	-20.61	0.03603	13.09	0.04469	16.08	0.02977
KUG 1203+206A	-18.10	0.03706	15.63	0.04521	14.97	0.02923
KUG 1203+206B	-18.61	0.03697	15.09	0.04505	14.94	0.03148
VV 062	-18.73	0.03704	14.91	0.04625	14.78	0.02950
SDSS J120621.91+203351.8	-18.15	0.03744	15.23	0.04622	12.66	0.02849
2MASX J12063969+2027235	-19.25	0.03716	14.47	0.04497	14.50	0.02896

Table 3.7: Colors and error of sample galaxies

Name	$B-V$	$\sigma(B-V)$	$B-R$	$\sigma(B-R)$	$V-R$	$\sigma(V-R)$
NGC 4098	1.34	0.05746	1.01	0.04602	-0.33	0.05300
NGC 4095	0.71	0.05745	0.93	0.04599	0.21	0.05299
NGC 4093	0.69	0.05760	0.90	0.04616	0.22	0.05305
NGC 4092	0.53	0.05743	0.69	0.04595	0.16	0.05299
NGC 4091	0.65	0.05739	0.88	0.04590	0.23	0.05297
NGC 4089	0.72	0.05739	0.94	0.04591	0.21	0.05297
NGC 4090	0.50	0.05741	0.66	0.04594	0.16	0.05300
NGC 4086	0.63	0.05741	-2.26	0.04674	-2.89	0.05370
KUG 1203+206A	0.25	0.05846	0.94	0.04720	0.69	0.05383
KUG 1203+206B	0.35	0.05828	0.55	0.04856	0.20	0.05496
VV 062	0.42	0.05925	0.61	0.04735	0.19	0.05486
SDSS J120621.91+203351.8	0.61	0.05948	3.26	0.04705	2.65	0.05429
2MASX J12063969+2027235	0.42	0.05833	0.44	0.04711	0.03	0.05348

3.5 B_{25} Diameter of the Sample Galaxies

The properties of B_{25} apertures bring on diameter of our sample galaxies. We obtained size of galaxies by multiply semi-major axis of apertures with average distance. The sample galaxy's diameters, including eccentricity and position angles obtained from the ESP package (Section 3) are listed in table 3.8 .

Table 3.8: The B_{25} diameters of the sample galaxies.

Name	Diameter (pc)	Eccentricity	Position angle (degree)
NGC 4098	15774.57	0.00	0
NGC 4095	15617.01	0.47	127
NGC 4093	11653.67	0.00	89
NGC 4092	16047.28	0.24	41
NGC 4091	19610.65	0.93	43
NGC 4089	12926.30	0.00	90
NGC 4090	18568.30	0.78	45
NGC 4086	15938.20	0.48	90
KUG 1203+206A	6005.61	0.28	115
KUG 1203+206B	10908.27	0.78	13
VV 062	11284.00	0.74	3
SDSS J120621.91+203351.8	10890.09	0.94	-15
2MASX J12063969+2027235	9696.24	0.80	16

3.6 Morphological Type of Galaxies

The sample galaxies were classified follow de Vaucouleurs's T-type system. An additional type, "11" was defined for spiral galaxies which are edge-on and do not clearly show structures. Furthermore, "pec" was used to remark for peculiar galaxies. The observation of this study shows that types of galaxies consist of 8 spiral, 4 elliptical and 1 irregular morphological types as shown in table 3.9. Three spiral and two elliptical galaxies are found to have peculiar structures. Some samples for each type of our sample galaxies are shown in figure 3.2.

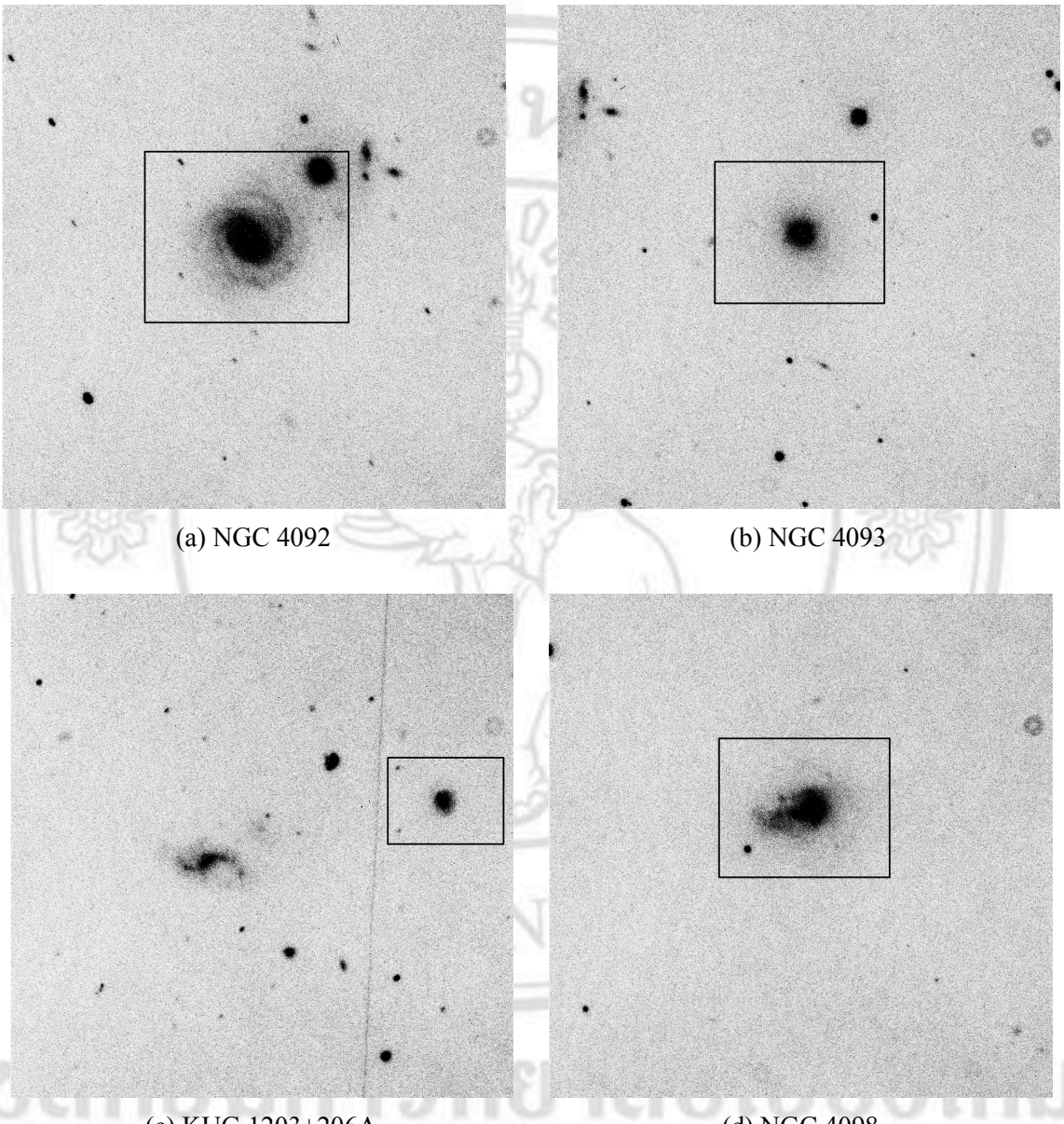

(a) NGC 4092 (b) NGC 4093

(c) KUG 1203+206A (d) NGC 4098

Figure 3.2: Morphological type some galaxies sample : NG C4092 is spiral galaxy (the upper-left panel), NGC 4093 is elliptical galaxy (the upper-right panel), KUG 1203+206A is irregular galaxy (the lower-left panel) and NGC 4098 is peculiar elliptical galaxy (the lower-right panel).

Table 3.9: Morphological type and T-type of sample galaxies.

Name	Type		T-Type
	SIMBAD	This work	
NGC 4098	S?	E0,pec	-5
NGC 4095	E	E1	-5
NGC 4093	E?	E0	-5
NGC 4092	Sa	Sab	2
NGC 4091	S	Sa	1
NGC 4089	E?	E0,pec	-5
NGC 4090	Sab	Sa	1
NGC 4086	S0	Sbc,pec	4
KUG 1203+206A	-	Irr	10
KUG 1203+206B	S	SBc	5
VV 062	Sb	Sbc,pec	4
SDSS J120621.91+203351.8	-	S?,pec	11
2MASX J12063969+2027235	S?	SBb	3

3.7 Calculation of Equivalent Width of Hα (EW(Hα))

Star formation of galaxies were studied in term of equivalent width of Hα. The observation for calculation of EW(Hα) were taken by two filters, one is [S II] filter and the other is Red-continuum filter.

3.7.1 CR ratio of continuum count and errors

CR ratio is parameter to correct count of continuum flux. It was estimated from ratio of counts of reference stars in the [S II] filter images to counts of the reference stars in the Red continuum filter images, as shown in the following equation :

$$CR_{\mathrm{i}} = \frac{C_{[\mathrm{S\,II}],\mathrm{S_i}}}{C_{\mathrm{Red},\mathrm{S_i}}}, \tag{3.25}$$

where CR_{i} is CR value of each reference star, $C_{[\mathrm{S\,II}],\mathrm{S_i}}$ is count or signal of reference star in the [S II] filter images and $C_{\mathrm{Red},\mathrm{S_i}}$ is count or signal of reference star in the Red continuum

filter images. Thus, the average value of CR ratio will be have got by

$$CR = \frac{\sum_{i=1}^{N} CR_{\rm i}}{N}, \tag{3.26}$$

that

$$\sigma(CR) = \sqrt{\frac{\sum_{i=1}^{N}(CR_{\rm i} - CR)^2}{N(N-1)}}, \tag{3.27}$$

where $\sigma(CR)$ is error of CR ratio and N is number of reference stars. Therefore, we calibrated continuum count of galaxies by

$$C_{\rm C} = CR \times C_{\rm Red,g}, \tag{3.28}$$

where $C_{\rm C}$ is continuum count of galaxies and $C_{\rm Red,g}$ is count of galaxy in Red continuum filter images. Error of $C_{\rm C}$ can be provided by

$$(\frac{\sigma(C_{\rm C})}{C_{\rm C}})^2 = (\frac{\sigma(CR)}{CR})^2 + (\frac{\sigma(C_{\rm Red,g})}{C_{\rm Red,g}})^2, \tag{3.29}$$

which

$$\sigma(C_{\rm Red,g}) = \sqrt{\frac{C_{\rm Red,g}}{k}}, \tag{3.30}$$

where $\sigma(C_{\rm C})$ is error of continuum counts, $\sigma(C_{\rm Red,g})$ is error of counts in Red continuum filter images and k is electron/ADU gain of Red continuum filter.

3.7.2 The Hα emission line counts and errors

Signal of galaxies from [S II] filter is the count of galaxies that contained count of the Hα emission line and continuum counts. Then, the equation (3.31) was applied to determine Hα emission line counts for all sample galaxies.

$$C_{\rm H\alpha} = C_{\rm [S\,II]} - C_{\rm C}, \tag{3.31}$$

where $C_{\rm H\alpha}$ is Hα emission line counts or Hα emission line signal of galaxies and $C_{\rm [S\,II]}$ is count of galaxies in [S II] filter images.

$$\sigma(C_{\rm H\alpha})^2 = \sigma(C_{\rm [S\,II]})^2 + \sigma(C_{\rm C})^2, \tag{3.32}$$

and

$$\sigma(C_{[\mathrm{S\,II}]}) = \sqrt{\frac{C_{[\mathrm{S\,II}]}}{k}}. \tag{3.33}$$

Errors of Hα emission line counts were determined by equation (3.32) and (3.33) where $\sigma(C_{\mathrm{H}\alpha})$ is error of Hα emission line counts, $\sigma(C_{[\mathrm{S\,II}]})$ is error of count of galaxies in [S II] filter images and k is electron/ADU gain of [S II] filter.

3.7.3 Equivalent width of Hα and signal to noise ratio

We studied star formation in galaxies which can be explained by using equivalent width of Hα, EW(Hα). The Hα emission line (6563 Å) used in this study, associates the [N II] emission lines (6548 and 6584 Å). Consequently, this study used Hα to represent Hα+[N II] emission lines. The equivalent width of Hα (EW(Hα)) was calculated by using the following equation [Gavazzi et al., 2006, Kriwattanawong et al., 2011]

$$EW(H\alpha) = \frac{\int T_n(\lambda)d\lambda}{T_{n(6563(1+z))}} \frac{C_{\mathrm{H}\alpha}}{C_{\mathrm{C}}} \tag{3.34}$$

where T_n is transmissivity of the [S II] filter and z is redshift of the galaxy. Significance of EW(Hα) was represented by signal to noise ratio value, S/N. The signal to noise ratio is the ratio of Hα emission counts to error of Hα count. In this study, we required the S/N value of sample galaxies more than 3.0, showing more than a 99% statistical significance, in order to confirm significant level of EW(Hα) values.

$$S/N = \frac{C_{\mathrm{H}\alpha}}{\sigma(C_{\mathrm{H}\alpha})}, \tag{3.35}$$

while

$$S/N = \frac{EW(H\alpha)}{\sigma(EW(H\alpha))}, \tag{3.36}$$

therefore

$$\sigma(EW(H\alpha)) = \frac{EW(H\alpha)}{S/N}, \tag{3.37}$$

where $\sigma(EW(H\alpha))$ is error of equivalent width of Hα. The results of our sample galaxies were shown in the table 3.10

Table 3.10: The equivalent width of Hα, errors and the signal to noise ratios.

Name	EW(Hα) (Å)	$\sigma(EW(H\alpha))$ (Å)	S/N
NGC 4098	12.146	0.903	13.452
NGC 4095	6.569	0.910	7.215
NGC 4093	7.555	0.910	8.300
NGC 4092	22.263	0.953	23.362
NGC 4091	15.008	0.904	16.610
NGC 4089	5.328	0.906	5.878
NGC 4090	22.432	0.907	24.743
NGC 4086	9.201	0.915	10.054
KUG 1203+206A	23.140	0.997	23.211
KUG 1203+206B	23.450	0.979	23.953
VV 062	12.038	0.954	12.613
SDSS J120621.91+203351.8	-9.631	0.949	-10.150
2MASX J12063969+2027235	17.764	0.933	19.037

3.8 Estimation of Mean Stellar Luminosity-Weighted Ages and Metallicities, $[Fe/H]$

During several decades, many researchers have proposed evolutionary stellar population synthesis models to predict spectral energy distributions of stellar populations. Theses models can be used to predict mean stellar ages and metallicities of various stellar systems. Accordingly, we can estimate mean stellar luminosity-weighted ages and metallicities of galaxies by using the population synthesis model of Pietrinferni et al. [2004] who studied star clusters and showed relations of them. The model grid shows feature of lines for synthesized ages and metallicities of large stellar populations, in form of color-color diagrams. We obtained near-infrared J and K magnitudes from the SIMBAD Astronomical Database. The grid models of Pietrinferni et al. [2004] offered constant age and metallicity lines which were plotted in color-color diagrams. The solid lines represent constant metallicity, $[Fe/H]$, ranging of -1.79, -1.27, -0.96, -0.66, and 0.06. The constant ages lines were represented by dotted lines for 1, 2, 3, 6, 10, and 14 Gyr. In this work, we used our BVR_c magnitudes for optical bands and JK near-infrared magnitudes from database to plot over the model grid. Therefore, the comparison between position of our sample galaxies and the lines have given mean stellar luminosity-weighted ages and metallicities value. Sample of the model grid is shown in figure 3.3.

Table 3.11: Near-infrared magnitudes of the sample galaxies collected from the SIMBAD Astronomical Database.

Name	J	H	K
NGC 4098	10.89	10.17	9.94
NGC 4095	11.07	10.34	10.14
NGC 4093	11.86	11.21	10.94
NGC 4092	11.44	10.79	10.51
NGC 4091	11.62	10.84	10.59
NGC 4089	11.38	10.67	10.40
NGC 4090	11.62	10.89	10.60
NGC 4086	11.60	10.90	10.57
KUG 1203+206B	14.73	13.66	13.89
2MASX J12063969+2027235	13.48	12.95	12.73

3.9 Estimation of Sample Galaxy Masses

Masses of sample galaxies were calculated following the relation between mass and luminosity of galaxies that was presented by Girardi et al. [2002]. Girardi et al. [2002] studied the relation by using the bisecting unweighted procedure. Girardi et al. [2002] presented mass to light ratio of galaxies in clusters, ranging from small groups to large clusters. The analysis gave linear fitting equation that show the relation between mass and luminosity of sample galaxies and show their masses were increasing faster than their luminosity. Thus, the relation was adapted to calculate mass of the sample galaxies as follow :

$$\frac{M}{M_{\odot}} = 10^{-1.596\pm0.381}(\frac{L_{\rm B}}{L_{\rm B,\odot}})^{1.338\pm0.033}, \tag{3.38}$$

where M is mass of galaxy, $M_{\odot}$ is the solar mass, $L_{\rm B}$ is luminosity of the galaxy in B band and $L_{\rm B,\odot}$ is the solar luminosity in the B band.

The luminosity of galaxies were calculated by using the fundamental photometry equation, i.e., the relation between magnitude, flux and luminosity.

$$B - B_{\odot} = -2.5\log(\frac{f_{\rm B}}{f_{\rm B,\odot}}), \tag{3.39}$$

that

$$f = \frac{L}{4\pi d^2}, \tag{3.40}$$

where $B_\odot$ is B magnitude of the sun, $f_{\rm B}$ is flux in B band of the galaxies, $f_{\rm B,\odot}$ is flux in B band of the sun and d is the average distance of galaxy group from the earth. Thus, we determined luminosity in B band of galaxies by using

$$L_{\rm B} = \frac{d^2 L_{\rm B,\odot}}{d_\odot^2} \exp\left(\frac{B - B_\odot}{-2.5} \ln 10\right), \tag{3.41}$$

where $L_{\rm B}$ is the luminosity in B band of galaxies, $L_{\rm B,\odot}$ is the luminosity in B band of the sun and $d_\odot$ is the distance of the sun from the earth. The error of the luminosity of galaxies were calculated by using equation (3.42). However, we assume error of $B_\odot$, $d_\odot$, d and $L_{\rm B,\odot}$ are negligible. Then, the error of the luminosity of the galaxies ($\sigma(L_{\rm B})$) can be estimated by using equation (3.43).

$$\sigma(L_{\rm B}) = \sqrt{(\frac{\partial L}{\partial d}\sigma(d))^2 + (\frac{\partial L}{\partial L_\odot}\sigma(L_\odot))^2 + (\frac{\partial L}{\partial d_\odot}\sigma(d_\odot))^2 + (\frac{\partial L}{\partial B}\sigma(B))^2 + (\frac{\partial L}{\partial L_{\rm B,\odot}}\sigma(L_{\rm B,\odot}))^2}, \tag{3.42}$$

$$\sigma(L_{\rm B}) = \sqrt{(\frac{\ln 10}{-2.5} L_{\rm B}\sigma(B))^2}. \tag{3.43}$$

Error of masses mainly come from three parameters, first is error of galaxy luminosity, second is error of power number -1.596 $\pm$ 0.381 and the other is error of power number 1.338 $\pm$ 0.033. However, we assumed that 1.338 is constant value because 0.033 is much smaller than 1.338, (0.033 $\ll$ 1.338). Finally, we obtained error of the mass of our sample galaxies ($\sigma(\frac{M}{M_\odot})$) from (3.44). The estimated masses and error were presented in table 3.12.

$$\sigma(\frac{M}{M_\odot}) = \sqrt{(\frac{M}{M_\odot}\frac{1.338}{L_{\rm B}}\sigma(L_{\rm B}))^2 + (\frac{M}{M_\odot} 0.381 \ln 10)^2} \tag{3.44}$$

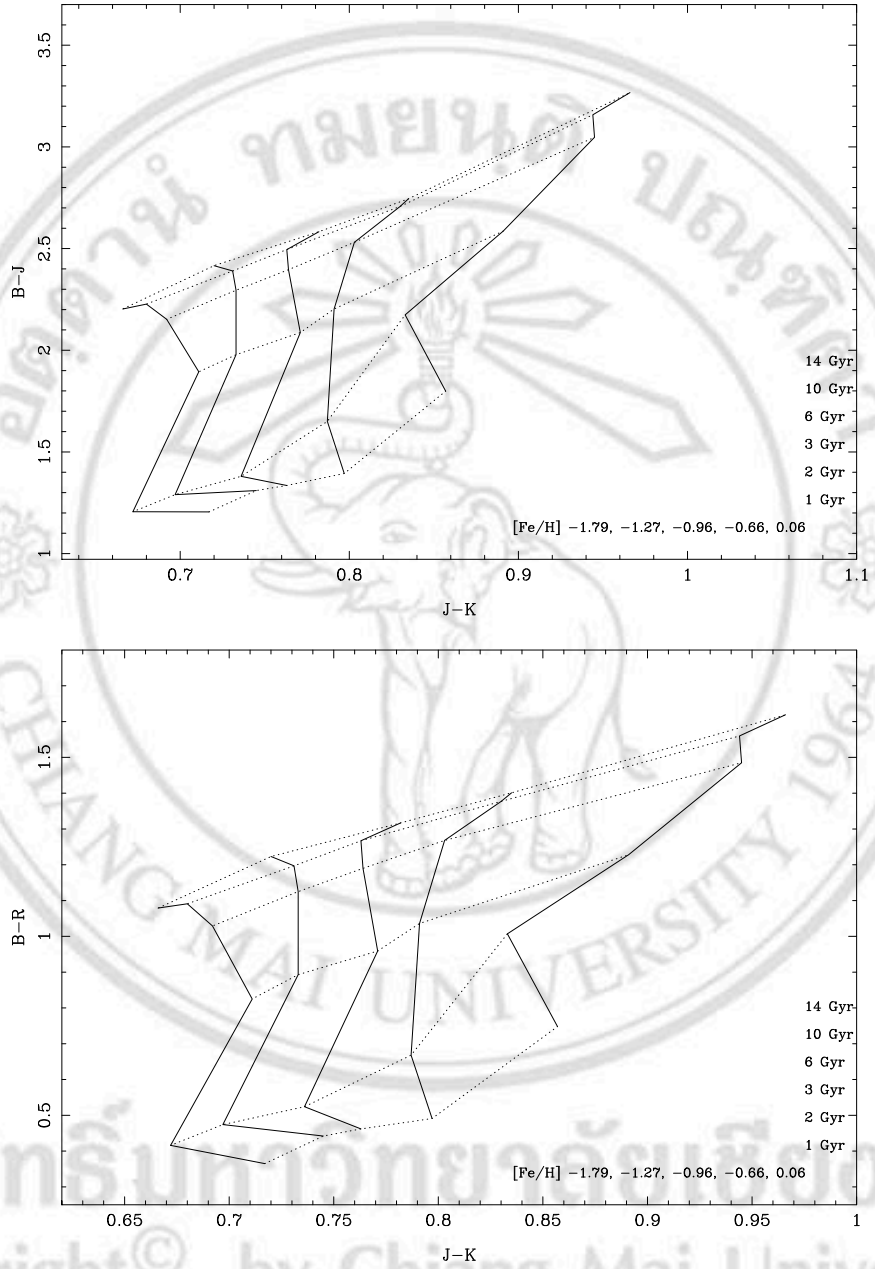

Figure 3.3: Sample of model grid of Pietrinferni et al. [2004] was plotted in color-color diagram, the upper panel shows the diagram plotted in $B - J$ vs $J - K$ and the lower panel shows the diagram plotted in $B - R$ vs $J - K$.

Table 3.12: The estimated mass and luminosity in B band of sample galaxies.

Name	$L_{\mathrm{B}}(\times 10^{36})$	$\sigma(L_{\mathrm{B}})(\times 10^{36})$	$M/M_{\odot}(\times 10^{12})$	$\sigma(M/M_{\odot})(\times 10^{12})$
NGC 4098	7.09	0.236	3.40	2.98
NGC 4095	6.55	0.218	3.05	2.68
NGC 4093	3.38	0.113	1.26	1.11
NGC 4092	7.84	0.261	3.89	3.42
NGC 4091	4.58	0.152	1.89	1.66
NGC 4089	5.32	0.176	2.31	2.03
NGC 4090	5.85	0.194	2.63	2.31
NGC 4086	5.30	0.176	2.30	2.02
KUG 1203+206A	0.53	0.018	0.10	0.09
KUG 1203+206B	0.84	0.029	0.20	0.17
VV 062	0.94	0.032	0.23	0.20
SDSS J120621.91+203351.8	0.55	0.019	0.11	0.10
2MASX J12063969+2027235	1.51	0.052	0.43	0.38